Luminescent assemblies of pyrene-containing bent-core mesogens: liquid crystals, π-gels and nanotubes

Marta Martínez-Abadía,[a]† Shinto Varghese,[b] †† Johannes Gierschner,*[b]
Raquel Giménez*[a]and M. Blanca Ros*[a]

[a] *Instituto de Nanociencia y Materiales de Aragón (INMA), Departamento de Química Orgánica-Facultad de Ciencias, Universidad de Zaragoza-CSIC, E-50009 Zaragoza, Spain.*
[b] *Instituto Madrileño de Estudios Avanzados en Nanociencia (IMDEA Nanociencia), Ciudad Universitaria de Cantoblanco, E-28049, Madrid, Spain.*
† Present address: POLYMAT, University of the Basque Country UPV/EHU, Avenida de Tolosa 72, E-20018 Donostia–San Sebastian, Spain.
†† Present address: School of Applied & Interdisciplinary Sciences, Indian Association for the Cultivation of science, 2A & 2B, Raja S.C. Mullick Road, Kolkata-700032, West Bengal, India.

Abstract: Bent-shaped molecules incorporating terminal pyrene moieties were designed and synthesized aiming at promoting a variety of luminescent self-assembled materials. The novel compounds are fluorescent both in solution and in condensed phases, achieving brighter fluorescence in the last case with fluorescence quantum yields up to 60%. Depending on the number of pyrene units (1 or 2) and/or the presence or absence of a long and flexible linker between the bent-core and the pyrene structures, bent-core liquid crystal phases, physical gels and nanoassemblies were obtained. Their properties depend on the molecular design, unveiling a synergistic and versatile 'tandem' of the bi-functional system in supramolecular functional materials chemistry. Long hydrocarbon spacers connecting bent-core and pyrene structures were necessary to display mesomorphic properties, achieving monotropic rectangular columnar mesophases, being for one compound stable at room temperature and displaying a glassy transition below room temperature, as revealed by POM, DSC and XRD. Liquid crystal phases exhibited excimer-like emission. In addition, organogels were obtained without the help of hydrogen bonding functionalities, exhibiting in one case supergelator behavior. Different nanoassemblies were obtained out of these non-amphiphilic bent-core structures, in particular unprecedented organic nanotubes with beveled ends formed by a single bilayer.

INTRODUCTION

Pyrene is a well-known organic chromophore that possesses remarkable photophysical and electronic properties,[1-5] as well as very attractive supramolecular capabilities.[4-9] This polycyclic aromatic hydrocarbon joints high fluorescence quantum yield of the monomer in solution and aggregated states, as well as efficient excimer emission for integration into devices such as OLEDs.[3] In addition, it is highly sensitive towards microenvironment changes,[10] being extensively used as probes either for biological purposes[11] to obtain structural and dynamic information on multi-molecular assemblies,[12-14] or for photonic devices.[15-18]

To succeed in these targets, two key features have been revealed essential for modulating functional performance and processability, namely appropriate molecular design and organization of the active motives. Therefore, a variety of pyrene-containing molecular structures, suitable for supramolecular arrangements, have been reported with the aim of self-organizing the pyrene moiety.[3] By using both intra- and intermolecular interactions, a number of strategies and bottom-up methodologies have been proposed to achieve the desired functional properties.[6-14] Thus, non-covalent interactions, including π–π stacking, van der Waals forces and hydrogen-bonds among others, are crucial to obtain programmed molecular building blocks that evolve into well-defined hierarchical responsive superstructures.[15-18] In this regard, physical gels and liquid crystalline phases have attracted especial attention. Gels,[9, 14, 19-22] through the spontaneous aggregation of pyrene-based small molecules or polymers as gelators, render into 1D fibrils, that are further entangled into a complex 3D network, in which a large amount of solvent can be immobilized. The so-called π-gels[23-24] can potentially provide the structural control required for low-cost and large-area liquid deposition

methods. On the other hand, liquid crystals[25-27] has provided a variety of classical layered or columnar anisotropic functional self-assemblies, also incorporating pyrene units,[28-38] keeping the order control to monitoring optical and electronic properties. However, only few suitable molecular design strategies providing both types of soft materials in the route to versatile functional materials have been published.[39-48]

Concerning mesophase organizations, bent-core liquid crystals (BCLC), which were discovered around 1996,[49] and their non-conventional mesophases have received significant attention in the soft matter area in the last decades.[50-57] Their compact packing has allowed the development of novel liquid crystal phases with polar, and in certain cases chiral arrangements, providing so far materials with very attractive functional properties.[54, 56, 58-61] Ferro- and antiferroelectric switching, piezoelectric or nonlinear optical responses from its polar molecular non-centrosymmetric order, have been reported even by using achiral molecules. Additionally, limited but striking luminescent bent-core type mesophases have also been afforded.[62-70] Interestingly, the combination of properties such as polarity, supramolecular chirality and luminescence endow bent-core liquid crystal phases with challenging opportunities in the context of chiral nanoarchitectonics.[71-73]

Efficient strategies to increase the potential for supramolecular arrangements of bent-core molecules have been developed by the incorporation of different structural motives in the same bent-shaped molecule. For this purpose, the use of dimers,[74] dendrimers[75-76] or hybrid molecules including bulky Si-containing moieties[77-81] or C60-units[82-83] have successfully essayed, paving the way to the possibility of stabilizing, even at room temperature, certain soft supramolecular order and obtaining interesting physical properties by controlling the nano-segregation and polar orientation of bent-core moieties.

Attractively, in the last years some authors have reported[48, 84-85] that the compact packing of the bent-shaped structures, which promotes BCLC, also occurs in the presence of a poor solvent, providing products ranging from single objects to supramolecular gels and, consequently, greatly increasing the charm and potential of bent-core molecules from academic and applied materials science interests.

Based on all these results and perspectives, we were attracted by the combination of bent-core molecules with the luminescent pyrene units. Thus, innovative and challenging designs of new photoactive functional materials and fluorescent probes for mesophase characterization could be proposed, as well as to explore the potential of the new pyrene-bent core building blocks to provide self-assembled materials keeping BCLC-like features at room temperature.

Herein, the supramolecular abilities of five bent-shaped molecules that incorporate the pyrene structure are analyzed aiming at promoting both bent-core liquid crystalline phases and supramolecular gels (Figure 1). In order to design bent-shaped molecules and induce BCLC, the well-known 3,4'-biphenylene system was selected as the central core. These compounds differ in the number of 1-pyrenebutyrate (Pyb) units (1 or 2) and in the presence or absence of a long and flexible linker between the bent-core structure (B) and the Pyb motif. Two di-pyrenebutyrates bent-shaped compounds, named Pyb-0-B-0-Pyb and Pyb-11-B-11-Pyb, without spacer (0) and with a spacer of 11 carbon atoms, respectively; two mono-substituted ones, Pyb-0-B and Pyb-11-B, as well as one product where the Pyb unit has been replaced for the 1-pyrenebutyramide (PybN), PybN-11-B, have been synthesized and characterized. The role of pyrene units and its proximity to the bent-core structure on the formation of bent-core mesophases and gels, and also to assess the photoluminescence of these newly supramolecular materials by studying the UV-Vis absorption and fluorescence are the main targets of our study. In addition, to check the key character of a bent-structure on these supramolecular trends and properties, a rod-like molecule, namely Pyb-11-C (C denotes the calamitic structure), has been incorporated in this structure-properties relationship study.

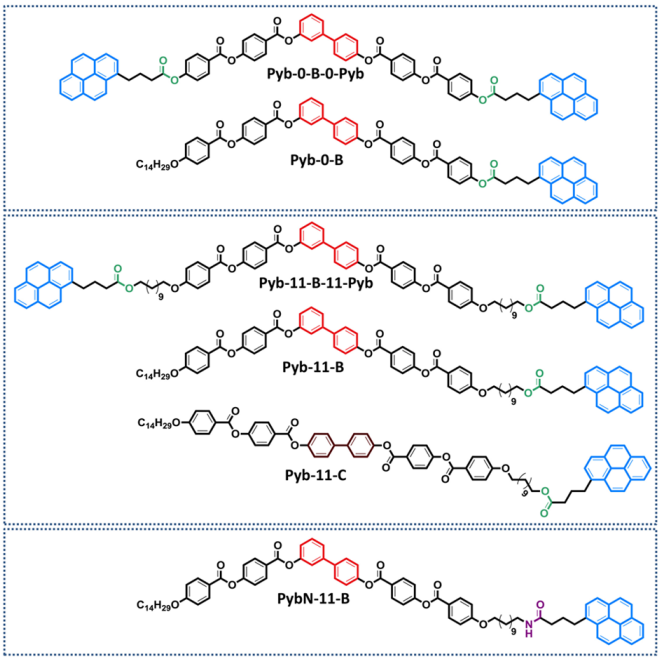

***Figure 1**. Chemical structure of the bent-shape and rod-like pyrene derivatives.*

RESULTS AND DISCUSSION

Synthesis.

The synthetic methods for the preparation of pyrenebutyrate and pyrenebutyramide derivatives are shown in Schemes S1-S6 in the ESI. Synthetic routes have been adapted from similar intermediates and they are based on Mitsunobu reactions and successive esterifications and deprotections of benzyl groups. All experimental details and structural characterization of the compounds are described in the Supporting Information.

Thermal and Liquid Crystalline Properties of the Compounds.

Phase transitions of the final target compounds were studied by polarizing optical microscopy (POM), differential scanning calorimetry (DSC) and X-ray diffraction (XRD). The transition temperatures, enthalpies and XRD data are gathered in Table 1. As it can be seen, only Pyb-11-B-11-Pyb, Pyb-11-B and Pyb-11-C, all with a long spacer, exhibit liquid crystalline properties.

Regarding bent-core compounds, Pyb-11-B was obtained as a crystal with a melting point of 110 °C and exhibits a mesophase in the cooling process with a spherulitic and pseudo focal-conic

***Table 1**. Thermal properties and XRD liquid crystal characterization data for the target compounds.*

Compound	Phase Transition T (°C) [ΔH (kJ mol^{-1})] [a, b]	Mesophase [T (°C) of XRD data]	d (Å)	Miller Index	Parameters (Å)
Pyb-0-B-0-Pyb	Cr 168 [41.1] [d] I I 143 [34.8] Cr Cr 168 [32.9][d] I	-	-	-	-
Pyb-11-B-11-Pyb	Cr 90 [76.2] [d] I I 69 [8.6] Col_r 6[c] Col_{rg} Col_{rg} 8 Col_r 75[c] [8.7] I	Col_r [rt][f]	57.8 29.8 24.3 19.3	101 002 602 303	a =230.3 c =59.7
Pyb-0-B	Cr 146 [45.1] [d] I I 111 [36.9] Cr Cr 145 [38.9] [d] I	-	-	-	-
Pyb-11-B	Cr 110 [76.2] [d] I I 103 [14.7] Col_r 65 [29.1] Cr Cr 110 [68.4] I	Col_r [102]	44.8 29.0 22.7	101 002 202	a =73.9 c =56.4
PybN-11-B	Cr 165 [60.1] I I 143 [60.5] [d] Cr Cr 164 [58.2] I	-	-	-	-
Pyb-11-C	Cr 158[c] [48.9] SmC 250[e] Dec SmC 154[c] [48.6] Cr Cr 157 [48.4] SmC 250[e] Dec	SmC [168]	43.5 21.8	001 002	c = 43.5

a) Data determined by DSC. Temperatures at the maximum of the peaks from first heating and cooling and second heating cycle at a scanning rate of 10 °C min^{-1}. Cr: crystal phase, SmC: smectic C mesophase, Colr: rectangular columnar mesophase, Col_{rg}: vitrified rectangular columnar mesophase I: Isotropic liquid. b) The crystal phase denoted as Cr is, in most cases, not unique (crystalline polymorphism). c) Onset data. d) Combined enthalpy of several crystalline transitions. e) Data obtained from POM. f) Determined at room temperature (rt) by cooling the sample quickly from the isotropic liquid.

texture (Figure 2). Pyb-11-B-11-PyB shows lower melting point and also a monotropic mesophase but with a different behaviour, as the liquid crystal phase remains stable without crystallizing during the following heating/cooling cycles and it shows a glass transition below room temperature. The diffraction patterns of mesophases for Pyb-11-B-11-Pyb and Pyb-11-B show several sharp reflections in the small angle region that do not correspond to lamellar structures, but can be attributed to a bent-core columnar mesophase with a rectangular unit cell (Col_r) (Figure 2).

Considering the planarity of pyrene unit that tends to be stacked with other pyrenes, and the close packing observed in BCLCs, significantly higher transition temperatures for these pyrene-bent-core derivatives than for the analogous bent-core compounds without pyrene-butyrate units would be expected. However, slightly lower melting points and enantiotropic liquid crystalline mesophases have been reported for bent-compounds without the pyrene groups,[86-87] while for the bent-core compounds studied here mesomorphism is not stabilized after melting. According to these results, the BCLC self-assembly seems to be distorted by the combination of long flexible spacers and pyrene terminal units.

Only in the cooling process from the isotropic liquid with higher molecular mobility, interactions can stabilize mesomorphism, but only in molecules with long flexible linkers connecting bent-core structures and pyrene unit.

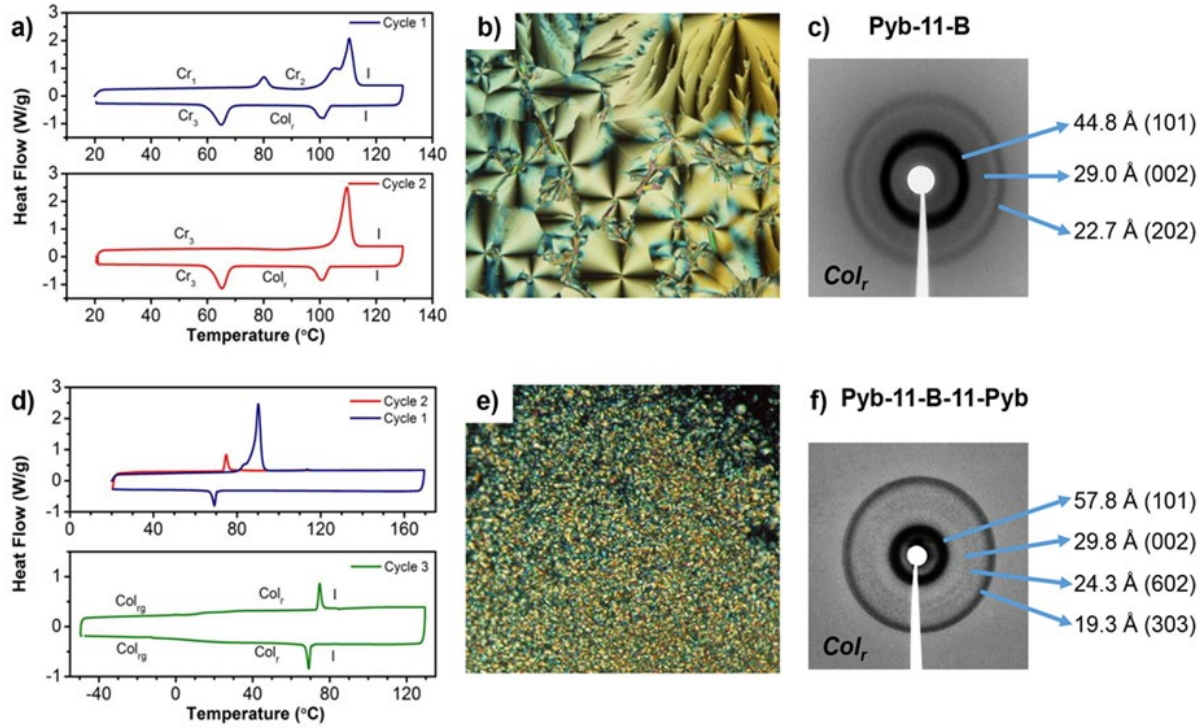

***Figure 2**. DSC thermograms, first and second heating/cooling cycles of Pyb-11-B (a) and Pyb-11-B-11-Pyb (d); POM textures of Pyb-11-B at 104 °C (Col_r phase) (b) and Pyb-11-B-11-Pyb at 74 °C (Col_r phase) (e); and XRD patterns of the mesophases of Pyb-11-B, Col_r phase at 102 °C (c) and Pyb-11-B-11-Pyb, Col_r phase at room temperature (f).*

In contrast, the rod-shaped compound Pyb-11-C melts above 155 °C and forms an enantiotropic SmC mesophase in a broad range of temperatures (around 100 °C) (Figure S7e, f). The diffraction pattern exhibits two reflections in the small angle, which are assigned to (001) and (002) of lamellar packing, which allows to calculate a spacing layer (43.5 Å), much lower than the theoretical molecular length (85.1 Å), suggesting the molecular tilt inside the smectic layer.

Photo-physics in Solution and in the Solid State.

The UV-Vis absorption spectra in dichloromethane (DCM) solution of these compounds exhibit distinct absorption bands. The sharp features in the 300-350 nm region correspond to the vibronics of the S0→S2 transition of pyrene,[88] and those < 280 nm to higher excited states of pyrene; the unstructured shoulder in the 280-300 nm region is assigned to biphenyl absorption of the angular bent-core (or rod-core) structure (Figure 3a, Table 2 and Table S1). Regardless of the spacer, the absorption spectra of the compounds with a single pyrene unit are similar in the spectral range above 300 nm, while in those with two pyrenes units, the pyrene absorption features approximately doubles. The fluorescence spectra of all compounds in dilute DCM solution exhibit structured monomer emission (Figure 3b), originating from the relaxed S1 state, with a maximum at 377 nm, and side bands at 397 and 418 nm of vibronic origin. The fluorescence quantum yields have been measured in solutions in air and the values are around 13-16 % (Table 2).[89]

In the condensed state of the compounds, the fluorescence was evaluated in different phases: the as-obtained solid (identified as pristine), processed solids, i.e. films cooled down from the mesophase at 10 °C min^{-1} (identified as scf) and liquid crystal phases (identified as LC or mesophase). In all spectra, excimer formation is observed, see Figures 3 and S8. Since dynamic excimer formation, as observed in solution,[2] can be excluded for the condensed phases, it can be concluded that the pyrenes generally, stack in the condensed phases. In the ampler definition of Birks, also such ground state complexes of pyrene are considered as excimers.[90] Exclusive excimer emission is observed for all mesophases as well as for the thermally treated samples (scf). A notable exception is Pyb-11-B, which shows significant monomer emission in the pristine state (~ 65% of the total fluorescence intensity; see Figure 3c and Table S2), giving rise to dual emission;[91] here, the monomer peak corresponds to that observed in solution (Figure 3a). Under thermal treatment the excimer content increases to 94%, and in the columnar mesophase only excimer emission is observed, see Figure 3c).

Some monomer emission is observed also in pristine Pyb-11-B-11-Pyb (~ 8%) (Figure 3d), which however disappears in the scf and mesophase. This result gives further evidence to our proposed scenario, that, when long spacers connect bent-core and pyrene structures, the intermolecular interactions significantly distort the pyrene packing. However, this is not the

Table 2. *UV-Vis and fluorescence data in dichloromethane (DCM) solution (in air) and as-obtained solid (pristine): Absorption and emission maxima (λ_{abs}, λ_{em}), fluorescence quantum yields (ΦF), and lifetimes (τF), radiative and non-radiative rates (k_r, k_{nr}).*

Compound	DCM solution		As-obtained solid (*Pristine*)				
	λ_{em} (nm)	Φ_F [a]	λ_{em} (nm)	Φ_F [b]	τ_F [c] (ns)	k_r [d] (s^{-1})	k_{nr} [d] (s^{-1})
Pyb-0-B-0-Pyb	377	0.16	478	0.58	94.4	$6.1 \cdot 10^6$	$4.4 \cdot 10^6$
Pyb-11-B-11-Pyb	377	0.13	475	0.55	57.0	$9.6 \cdot 10^6$	$7.9 \cdot 10^6$
Pyb-0-B	377	0.13	476	0.60	42.9	$1.4 \cdot 10^7$	$9.3 \cdot 10^6$
Pyb-11-B	377	0.14	377, 391, 397, 412	0.59	53.1	$1.1 \cdot 10^7$	$7.3 \cdot 10^6$
PybN-11-B	377	0.14	449	0.19	16.2	$1.2 \cdot 10^7$	$5.0 \cdot 10^7$
Pyb-11-C	377	0.15	470	-	-	-	-

a) From relative measurements using 9,10-diphenylanthracene in cyclohexane as reference (ΦF = 0.9). b) From absolute measurements in an integrating sphere. c) Intensity averages from bi and tri-exponential fits (see Table S3). d) From $\tau F = 1/(k_r + k_{nr})$, $\Phi F = k_r \cdot \tau F$.

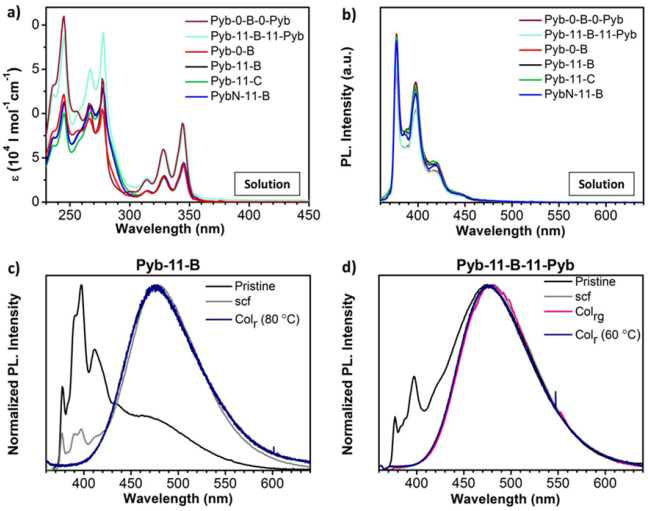

Figure 3. *a, b) Absorption and fluorescence spectra, respectively, of final compounds in dichloromethane (DCM) solutions (see also Table 2). The original fluorescence spectra have been divided by absorbance at the excitation wavelength for better comparison. c, d) Fluorescence spectra in different neat samples of Pyb-11-B and Pyb-11-B-11-Pyb. Pristine powder (black), scf: slow cooled film at 10 °C min^{-1} (grey), Colr: rectangular columnar mesophase (dark blue); Colrg: glassy rectangular columnar mesophase (pink).*

case for 1-pyrenebutyramide compound, PybN-11-B (Figure S8g), showing an excimer emission in all solid phases, being however blue-shifted by ~ 30 nm with respect to the excimer bands of the other compounds. Most probably, this is associated to a different arrangement of the pyrene units, due to a competitive/cooperative intermolecular H-bonding and π–π interaction balance.[31, 92] In fact, excimer band shape and spectral position (as well as intensity) are expected to be very sensitive to the precise position (separation, lateral displacement, rotation) of adjacent π–stacked molecules.[93-96]

Remarkably, the fluorescence quantum yields Φ_F of the pristine films of the 1-pyrenebutyrate compounds are all high with *ca*. 60% (Table 2), despite excimer formation. In fact, excimers are often assumed to be little emissive due to the vanishing oscillator strength of the emissive state (resulting in a low radiative rate k_r).[97] However, the resulting Φ_F is always decided by the competition of k_r with the non-radiative rate k_{nr},[98] so that pyrene excimers can be highly emissive in the crystalline[99] and liquid crystalline state.[28] We therefore measured the excimer lifetimes, giving about [42-94] ns in the pristine state, see Table 2. The rate constant analysis (Table 2) reveals that k_r is indeed small with *ca*. 1.10^7 s^{-1}, but can easily compete with k_{nr}, which is effectively suppressed in solid environments.[100] It is anyway noted that the excimer lifetimes exhibit a non-exponential behaviour (for details, see Table S3 and Figure S9),[101] which is ascribed to slightly different geometrical arrangements of the pyrene excimers due to non-negligible

disorder in the pristine samples. Finally, the pristine PybN-11-B excimer shows a much lower quantum yield (19%). This is however not due to a lower k_r (which is essentially the same like in the other compounds), but due to a higher k_{nr}, indicating again a different and less restrictive environment in the case of the compound with the amide group.

Gelation Properties and Photophysics in the Gel State.

Pyrene derivatives have been very often used to produce luminescent gels with different applications,[4, 9, 15, 102-104] most of them mediated by hydrogen bonding.[4, 15, 23, 105] On the other hand, few but consistent studies proved the ability of bent-core compounds as gelators.[48, 84, 106-107] In our case, the presence of an aromatic core (pyrene) and a bent-core structure prompted us to check their gelation abilities by π-π stacking in various polar or nonpolar, protic or aprotic solvents, namely 1-butanol, 1-octanol, toluene, nitrobenzene and chlorobenzene (see Table S4). For gelation tests, the mixture was heated until the solid was completely dissolved and the resulting clear solution was cooled in air to room temperature. The gel formation criteria used was to verify the absence of flowing of the solution when the test tube was turned upside-down at room temperature. Due to the low solubility of the di-substituted compounds, Pyb-11-B-11-Pyb and Pyb-0-B-0-Pyb, in the selected solvents, we limited our study to the gelation properties of compounds with only one pyrene unit, Pyb-0-B, Pyb-11-B, PybN-11-B and Pyb-11-C.

Interestingly, Pyb-bent core derivatives are suitable gelators of aliphatic alcohols such as 1-butanol or 1-octanol, giving rise to opaque gels (Figure 4c). Attractively, for this family of bent-shaped compounds, the presence of an amide group is not essential for the gelation. Moreover, the lowest critical gelation concentration (0.3 % w/w) has been reached for compound Pyb-11-B, acting as a supergelator. On contrast, PybN-11-B only can gelate 1-octanol at higher concentrations (10 % w/w), being, on the other hand, the solely gelator for aromatic

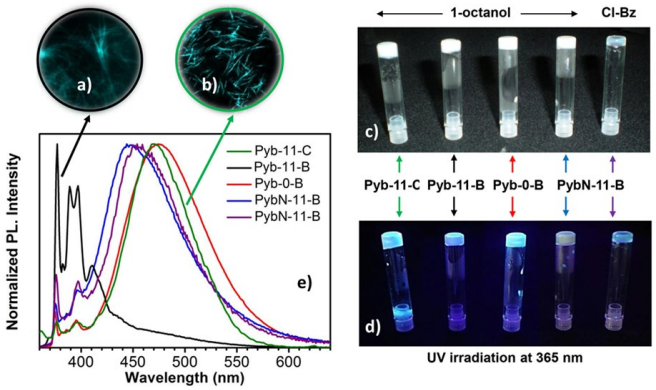

Figure 4. *Fluorescence microscopy images of xerogels of Pyb-11-B (a) and Pyb-11-C (b) irradiated at 385-400 nm. Photography of gels of Pyb-11-B (10% w/w, black line), Pyb-0-B (10% w/w, red line), Pyb-11-C (5% w/w, green line), PybN-11-B (10% w/w, blue line) in 1-octanol, and PybN-11-B (10% w/w, purple line) in chlorobenzene, all under room light (c) and UV light irradiation (d). Fluorescence spectra of the gels (e).*

solvents such as nitrobenzene or chlorobenzene, leading to transparent gels (Figure 4c). All these organogels exhibit thermally reversible sol-to-gel phase transitions; furthermore, upon UV irradiation, these gels exhibit strongly luminescent (Figure 4d), keeping the attractive optical features of the pyrene unit. Fluorescence microscopy allowed to visualize the luminescent network (Figures 4a and 4b).

Fluorescence measurements (Figure 4 and Table S5) show that the emission properties of the gels strongly depend on the chemical structure of the gelator, namely the length of the spacer and the nature of the linkage (ester vs amide) connecting pyrene and bent-core moieties (Figure 4e). In general, the gel emissions are similar to the optical properties evaluated for the pristine samples of gelators. In 1-octanol, all gels show excimer formation; an exception is again Pyb-11-B, which displays dual emission of the monomer and excimer bands similar to the as-obtained solid, but with different relative intensities. Evidently, the pyrene stacking is not sufficient to act as a driving force for gel formation; this is ascribed to the combination of the presence of only one pyrene unit, and the long flexible spacer, which only partly allows for excimer formation. This supports our proposal to explain the poor liquid crystal properties and monomeric fluorescence of Pyb-11-B.

In contrast, through the participation of H-bonds promoting the stacking of pyrene-moieties, PybN-11-B-based gels in 1-octanol exhibit also a blue-shifted excimer emission with lower lifetime (Table S5 and Figure S10).

The morphology of the network-structure of the xerogels was examined by scanning electron microscopy (SEM). Figure 5 shows the electron micrographs of the xerogels deposited on glass slides from different gels in 1-octanol, and in chlorobenzene for PybN-

11-B. The micromorphology of the aggregates and networks of gels is strongly dependent on the gel concentration, except for Pyb-0-B, and on the nature of the gelated solvent.

The xerogel morphology of Pyb-0-B in 1-octanol is formed by entangled nanotubes (Figure 5a and 5b) with outer diameters in the range of 80-125 nm for the gels at 10% w/w and inner diameters around 3 nm, while in the lower gelation concentration (2.5% w/w) two different sizes have been observed (30-40 and 80-100 nm). Interestingly, the gel in 1-octanol of this non-mesomorphic compound shows a lamellar structure, as revealed by XRD of the bulk, with multiple periodic reflections (Figure 6a); this is in fact similar to the molecular organization reported for the SmCP mesophase. In this case, the measured layer spacing by XRD (106 Å) is larger than the molecular length of the gelator (68 Å). This difference in layer spacing can be explained by the formation of a tilted bilayer in which two molecules are arranged in an antiparallel fashion and partially interdigitated through interacting pyrene units (estimated value: 126 Å) (Figure 6b), which is in accordance with the observed excimeric emission. Interestingly, Pyb-0-B has a strong tendency to form nanotubes and the formation of this tubular structure has also been detected by TEM at lower concentrations (0.1% w/w) (Figure 5i), showing outer diameters in the range of 30 nm (Figure 6c). As it can be seen from TEM images, all these nanotubes exhibit beveled ends with measured walls in the range of 10 nm. This is in accordance with the layer spacing measured by XRD, and indicates that the nanotube walls are formed by a single bilayer.

These self-assembled nanotubes are indeed new forms of soft matter nanotubes (SMNTs); the latter is a current challenging topic in the area of materials chemistry.[108-111] In this case, by using bent-core molecules without hydrophilic and hydrophobic segments, well-defined nanotubes can be easily obtained.

For compound Pyb-11-B in 1-octanol, the morphology of the aggregates varies with the concentration of gelator, noting at the highest concentration (10% w/w) large sheets that fold (Figure 5c), while at the minimum concentration (0.3% w/w) long flat ribbons are observed (Figure 5d). The XRD study of the gel has demonstrated that the sheets exhibit a defined crystalline structure, with multiple reflections in the small and wide angle and without a lamellar order. TEM studies of the aggregates, produced below the critical gelation concentration (0.1% w/w), showed that nanobelts (w: 100 - 400 nm) are formed by aggregation of initial nanofibers (w: 30 nm) (Figure 5j).

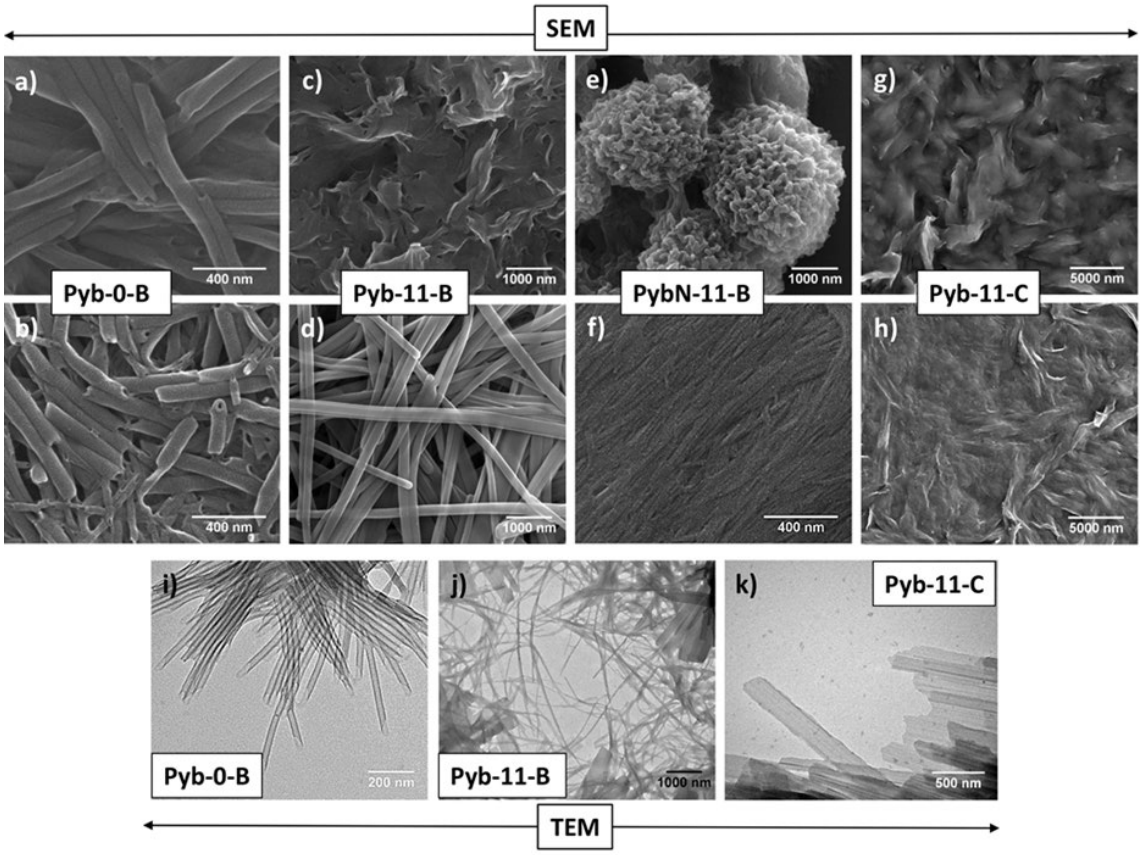

Figure 5. *SEM images of xerogels of: a, b) Pyb-0-B in 1-octanol (10% and 2.5% w/w, respectively); c, d) Pyb-11-B in 1-octanol (10% and 0.3% w/w, respectively); e) PybN-11-B in 1-octanol (10 % w/w); f) and PybN-11-B in chlorobenzene (10% w/w); and g, h) Pyb-11-C in 1-octanol (5% and 0.8% w/w, respectively). TEM images of aggregates: i) Pyb-0-B in 1-octanol (0.1% w/w); j) Pyb-11-B in 1-octanol (0.1% w/w); k) Pyb-11-C in 1-octanol (0.2% w/w).*

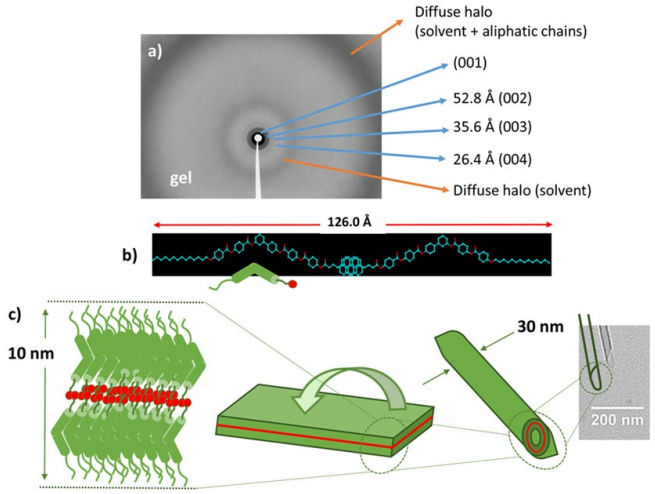

Figure 6. *XRD pattern of Pyb-0-B gel in 1-octanol (10% w/w) (a). Representation of proposed structural repeating unit forming the gel Pyb-0-B and its theoretical molecular length (b), and schematic representation proposed for the self-assembling tubular formation process.*

Concerning the organogels of PybN-11-B, both soft materials gelling 1-octanol and chlorobenzene have been evaluated, which demonstrate that the morphology of the aggregates of the gel network depends on the solvent. When chlorobenzene is used, compact nanofibers (Figure 5f) with a crystalline order can be observed (Figure S11c). On the other hand, using 1-octanol as solvent, laminar structures appear creased and entangled, giving rise to balls (Figure 5e). In this case, a liquid crystalline-like lamellar organization has been determined again by XRD (see Figure S11a-b), with a layer spacing (99.5 Å), larger than the molecular length (83.9 Å); this suggests a tilted bilayer order, favouring excimer pyrene-pyrene interactions.
Finally, for Pyb-11-C, self-assembled morphologies in the gels could not be clearly identified by SEM (Figure 5g-h); however, TEM investigations suggest the presence of sheets with a high
tendency for aggregation (Figure 5k). The XRD studies of these gels have shown a lamellar structure for the aggregates, very similar to the molecular assembly in the liquid crystal phase of this compound. However, a larger layer spacing (61.6 Å) (Figure S11d) was found here, suggesting similar molecular organization in both supramolecular materials, both allowing for excimer formation but in a more tilted disposition in the gel.

Comparing the gels based on both rod-core Pyb-11-C and the bent-core Pyb-11-B isomers, we can conclude that both render fluorescent gels, but the bent-core structure prevents the formation of excimeric emission as well as it provides suitable assemblies towards the generation of homogenous and defined fibers, even at higher concentrations of gelator.

Conclusions

The supramolecular abilities of five bent-shaped molecules, which incorporate pyrene moieties, were investigated, aiming at promoting both bent-core liquid crystalline phases and supramolecular gels. Interestingly, by changing the number of 1-pyrenebutate units (1 or 2) and/or the presence or absence of a long and flexible linker between the bent-core structure and the pyrene motif, a variety of supramolecular materials can be achieved; the resulting properties depend on the molecular design, unveiling a synergistic and versatile 'tandem' of the bi-functional system in supramolecular functional materials chemistry.

Bent-core and pyrene combination limit the formation of mesophases as only compounds with a long spacer between them leads to monotropic columnar mesophases, interestingly around room temperature and with a glass transition, leading to a glassy mesophase-like organization. However, this tandem is more effective on solvent-mediated self-assembly, as either attractive nanoaggregates or gelation in certain organic solvents, even without amide bonds, are promoted as alternatives to liquid crystals. Molecular aggregations afford fibrillar and tubular morphologies through a liquid-crystalline-like lamellar organization of the molecules, with formation of beveled nanotubes formed by a single bilayer.

In the absence of strong supramolecular driven-interactions, long hydrocarbon spacers connecting bent-core and pyrene structures seems to allow the dilution of the pyrene fragment in the apolar environment, hindering either excimer and thermotropic liquid crystal formation, in contrast to linear isomers. Nevertheless, pyrene attractively transfers fluorescent properties always to all these supramolecular materials with quantum yields in the condensed phases of up to 60%.

Based on all these results and considering the singular design and functional potentials of these two structural motives, the combination of bent-core and pyrene units opens broad and innovative research possibilities for challenging functional materials to explore. Using pyrene-bent core-based building blocks, a number of self-assembled materials which keep BCLC-like features at room temperature, to form gels and nanoaggregates including tubular architectures, can be certainly proposed. Nevertheless, further opportunities, so far unexplored for this sort of molecules, are envisaged; this includes vibrant research fields such as optics, optoelectronic and molecular electronics.

Author Contributions

The manuscript was written through contributions of all authors. All authors have given approval to the final version of the manuscript.

Conflicts of interest

There are no conflicts to declare.

Acknowledgements

The authors from INMA greatly appreciate financial support from projects of the Spanish Government PGC2018-093761-B-C31 [MCIU/AEI/FEDER, UE] and MAT2015-66208-C3-1 [MINECO/FEDER, UE], the Gobierno de Aragón/FEDER (research group E47_20R) and the JAE.PREDOC-CSIC (M. M-A) fellowship program. Thanks are given to the nuclear magnetic resonance, mass spectrometry, and thermal analysis services of the INMA (Univ. Zaragoza-CSIC), the LMA (Univ. Zaragoza) for TEM images and Servicio General de Apoyo a la Investigación-SAI (Univ. Zaragoza) for SEM images. The work at IMDEA was supported by the Spanish Government (MINECO-FEDER project CTQ2017-87054, MICINN project CEX2020-001039-S) and by the Campus of International Excellence (CEI) UAM+CSIC. We thank H. Bolink, Valencia, for access to the integrating sphere.

Notes and references

1. J. B. Birks and L. G. Christophorou, *Spectrochimica Acta*, 1963, **19**, 401-410.
2. F. M. Winnik, *Chem. Rev.*, 1993, **93**, 587-614.
3. T. M. Figueira-Duarte and K. Müllen, *Chem. Rev.*, 2011, **111**, 7260-7314.
4. S. M. M. Reddy, P. Dorishetty, G. Augustine, A. P. Deshpande, N. Ayyadurai and G. Shanmugam, *Langmuir*, 2017, **33**, 13504-13514.
5. S. Yang, Q. Liu, J. Ren and S. Ling, *Giant*, 2021, **5**, 100044.
6. M. El Idrissi, S. J. Teat, P. F. X. Corvini, M. J. Paterson, S. J. Dalgarno and P. Shahgaldian, *Chem. Commun.*, 2017, **53**, 1973-1976.
7. Y. Wu, H. Fan, C. Yang and L. Zhang, *Colloids Surf. A Physicochem. Eng. Asp.*, 2020, **585**, 124111.
8. M. Garrido, E. Martínez-Periñán, J. Calbo, L. Rodríguez-Pérez, J. Aragó, E. Lorenzo, E. Ortí, N. Martín and M. Á. Herranz, *J. Mater. Chem. C*, 2021, **9**, 10944-10951.
9. X. Bai, Y. Jiang, G. Zhao, J. Jiang, C. Yuan and M. Liu, *Soft Matter*, 2021, **17**, 4328-4334.
10. K. Kalyanasundaram and J. K. Thomas, *J. Am. Chem. Soc.*, 1977, **99**, 2039-2044.
11. P.-P. He, X.-D. Li, L. Wang and H. Wang, *Acc. Chem. Res.*, 2019, **52**, 367-378.
12. A. Méndez-Ardoy, A. Bayón-Fernández, Z. Yu, C. Abell, J. R. Granja and J. Montenegro, *Angew. Chem. Int. Ed.*, 2020, **59**, 6902-6908.
13. A. O. Ba-Salem and J. Duhamel, *Langmuir*, 2021, **37**, 6069-6079.
14. Y.-X. Li, L. Xu, S.-M. Kang, L. Zhou, N. Liu and Z.-Q. Wu, *Angew. Chem. Int. Ed.*, 2021, **60**, 7174-7179.
15. C. Madhu, B. Roy, P. Makam and T. Govindaraju, *Chem. Commun.*, 2018, **54**, 2280-2283.
16. D. Niu, Y. Jiang, L. Ji, G. Ouyang and M. Liu, *Angew. Chem. Int. Ed.*, 2019, **58**, 5946-5950.
17. Q. Wang, Q. Zhang, Q.-W. Zhang, X. Li, C.-X. Zhao, T.-Y. Xu, D.-H. Qu and H. Tian, *Nat. Commun.*, 2020, **11**, 158.
18. M. Pan, R. Zhao, B. Zhao and J. Deng, *Macromolecules*, 2021, **54**, 5043-5052.
19. J. H. van Esch and B. L. Feringa, *Angew. Chem. Int. Ed.*, 2000, **39**, 2263-2266.
20. N. M. Sangeetha and U. Maitra, *Chem. Soc. Rev.*, 2005, **34**, 821-836.
21. M. George and R. G. Weiss, *Acc. Chem. Res.*, 2006, **39**, 489-497.
22. S. Panja and D. J. Adams, *Chem. Soc. Rev.*, 2021, **50**, 5165-5200.
23. S. S. Babu, V. K. Praveen and A. Ajayaghosh, *Chem. Rev.*, 2014, **114**, 1973-2129.
24. S. Ghosh, V. K. Praveen and A. Ajayaghosh, *Annu. Rev. Mater. Res.*, 2016, **46**, 235-262.
25. E.-K. Fleischmann and R. Zentel, *Angew. Chem. Int. Ed.*, 2013, **52**, 8810-8827.
26. T. Kato, J. Uchida, T. Ichikawa and T. Sakamoto, *Angew. Chem. Int. Ed.*, 2018, **57**, 4355-4371.
27. T. Kato, M. Gupta, D. Yamaguchi, K. P. Gan and M. Nakayama, *Bull. Chem. Soc. Jpn.*, 2021, **94**, 357-376.
28. A. Hayer, V. de Halleux, A. Köhler, A. El-Garoughy, E. W. Meijer, J. Barberá, J. Tant, J. Levin, M. Lehmann, J. Gierschner, J. Cornil and Y. H. Geerts, *J. Phys. Chem. B*, 2006, **110**, 7653-7659.
29. K. P. Gan, M. Yoshio and T. Kato, *J. Mater. Chem. C*, 2016, **4**, 5073-5080.

30. Y. Sagara, C. Weder and N. Tamaoki, *Chem. Mater.*, 2017, **29**, 6145-6152.
31. M. Park, D.-G. Kang, Y.-J. Choi, W.-J. Yoon, J. Koo, S.-H. Park, S. Ahn and K.-U. Jeong, *Chem. Eur. J.*, 2018, **24**, 9015-9021.
32. H. Anetai, K. Sambe, T. Takeda, N. Hoshino and T. Akutagawa, *Chem. Eur. J.*, 2019, **25**, 11233-11239.
33. S. Irla, M. Pruthvi, V. A. Raghunathan and S. Kumar, *Dyes Pigments*, 2021, **194**, 109574.
34. B. Yao, G. Zhao, H. Wu, C. Mo, Z. Meng, C. Luo, S. Wang, T. Chen, Y. Fu, Y. Chen and P. Lin, *J. Lumin.*, 2021, **239**, 118329.
35. T. M. S. K. Pathiranage, Z. Ma, C. M. Udamulle Gedara, X. Pan, Y. Lee, E. D. Gomez, M. C. Biewer, K. Matyjaszewski and M. C. Stefan, *ACS Omega*, 2021, **6**, 27325-27334.
36. B. Yao, Z. Huang, P. Lin, L. Li, S. Wang, G. Gong, Y. Chen, L. Dong, X. Wang and Y. Zang, *Liq. Cryst.*, 2021, **48**, 1087-1094.
37. R. Walker, M. Majewska, D. Pociecha, A. Makal, J. M. Storey, E. Gorecka and C. T. Imrie, *ChemPhysChem*, 2021, **22**, 461-470.
38. B. A. G. Lamers, M. H. C. van Son, F. V. de Graaf, B. W. L. van den Bersselaar, B. F. M. de Waal, K. Komatsu, H. Sato, T. Aida, J. A. Berrocal, A. R. A. Palmans, G. Vantomme, S. C. J. Meskers and E. W. Meijer, *Mater. Horizons*, 2022, **9**, 294-302.
39. J. J. van Gorp, J. A. J. M. Vekemans and E. W. Meijer, *J. Am. Chem. Soc.*, 2002, **124**, 14759-14769.
40. S. Yagai, T. Kinoshita, M. Higashi, K. Kishikawa, T. Nakanishi, T. Karatsu and A. Kitamura, *J. Am. Chem. Soc.*, 2007, **129**, 13277-13287.
41. K. Takashi and T. Kana, *Chem. Lett.*, 2009, **38**, 634-639.
42. S. Diring, F. Camerel, B. Donnio, T. Dintzer, S. Toffanin, R. Capelli, M. Muccini and R. Ziessel, *J. Am. Chem. Soc.*, 2009, **131**, 18177-18185.
43. F. Aparicio, F. García and L. Sánchez, *Chem. Eur. J.*, 2013, **19**, 3239-3248.
44. N. Saito, K. Kanie, M. Matsubara, A. Muramatsu and M. Yamaguchi, *J. Am. Chem. Soc.*, 2015, **137**, 6594-6601.
45. D. Görl, B. Soberats, S. Herbst, V. Stepanenko and F. Würthner, *Chem. Sci.*, 2016, **7**, 6786-6790.
46. B. Pradhan, V. M. Vaisakh, G. G. Nair, D. S. S. Rao, S. K. Prasad and A. A. Sudhakar, *Chem. Eur. J.*, 2016, **22**, 17843-17856.
47. A. P. Sivadas, D. S. S. Rao, N. S. S. Kumar, D. D. Prabhu, S. Varghese, C. N. Ramachandran, R. M. Ongungal, S. Krishna Prasad and S. Das, *J. Phys. Chem. B*, 2017, **121**, 1922-1929.
48. M. Castillo-Vallés, A. Martínez-Bueno, R. Giménez, T. Sierra and M. B. Ros, *J. Mater. Chem. C*, 2019, **7**, 14454-14470.
49. T. Niori, T. Sekine, J. Watanabe, T. Furukawa and H. Takezoe, *J. Mater. Chem.*, 1996, **6**, 1231-1233.
50. R. A. Reddy and C. Tschierske, *J. Mater. Chem.*, 2006, **16**, 907-961.
51. H. Takezoe and Y. Takanishi, *Jpn. J. Appl. Phys.*, 2006, **45**, 597-625.
52. A. Eremin and A. Jákli, *Soft Matter*, 2013, **9**, 615-637.
53. C. Tschierske, *Angew. Chem. Int. Ed.*, 2013, **52**, 8828-8878.
54. J. W. Goodby, P. J. Collings, T. Kato, C. Tschierske, H. Gleeson and P. Raynes, eds., *Handbook of Liquid Crystals*, Wiley-VCH, Weinheim, 2014.
55. C. Tschierske and G. Ungar, *ChemPhysChem*, 2016, **17**, 9-26.
56. H. Takezoe, *Mol. Cryst. Liq. Cryst.*, 2017, **646**, 46-65.
57. J. Liu, S. Shadpour, M. E. Prévôt, M. Chirgwin, A. Nemati, E. Hegmann, R. P. Lemieux and T. Hegmann, *ACS Nano*, 2021, **15**, 7249-7270.
58. J. Etxebarria and M. B. Ros, *J. Mater. Chem.*, 2008, **18**, 2919-2926.
59. M. Martínez-Abadía, R. Giménez and M. B. Ros, *Adv. Mater.*, 2018, **30**, 1704161.
60. K. I. Shivakumar, D. Pociecha, J. Szczytko, S. Kapuściński, H. Monobe and P. Kaszyński, *J. Mater. Chem. C*, 2020, **8**, 1083-1088.
61. W. Park and D. K. Yoon, *Crystals*, 2020, **10**, 675.
62. R. Deb, R. K. Nath, M. K. Paul, N. V. S. Rao, F. Tuluri, Y. Shen, R. Shao, D. Chen, C. Zhu, I. I. Smalyukh and N. A. Clark, *J. Mater. Chem.*, 2010, **20**, 7332-7336.
63. R. Deb, A. R. Laskar, D. D. Sarkar, G. Mohiuddin, N. Chakraborty, S. Ghosh, D. S. Shankar Rao and N. V. S. Rao, *CrystEngComm*, 2013, **15**, 10510-10521.
64. R. Deb, M. Oneill, N. V. S. Rao, N. A. Clark and I. I. Smalyukh, *ChemPhysChem*, 2014, **16**, 243-255.
65. M. K. Paul, P. Paul, S. K. Saha and S. Choudhury, *J. Mol. Liq.*, 2014, **197**, 226-235.
66. R. Deb, M. Oneill, N. V. S. Rao, N. A. Clark and I. I. Smalyukh, *ChemPhysChem*, 2015, **16**, 243-255.
67. M. Martinez-Abadia, B. Robles-Hernandez, B. Villacampa, M. R. de la Fuente, R. Gimenez and M. B. Ros, *J. Mater. Chem. C*, 2015, **3**, 3038-3048.
68. M. Martinez-Abadia, S. Varghese, B. Milian-Medina, J. Gierschner, R. Gimenez and M. B. Ros, *Phys. Chem. Chem. Phys.*, 2015, **17**, 11715-11724.
69. M. Martínez-Abadía, B. Robles-Hernández, M. R. de la Fuente, R. Giménez and M. B. Ros, *Adv. Mater.*, 2016, **28**, 6586-6591.
70. M. Martínez-Abadía, S. Varghese, P. Romero, J. Gierschner, R. Giménez and M. B. Ros, *Adv. Opt. Mater.*, 2017, **5**, 1600860.
71. K. V. Le, H. Takezoe and F. Araoka, *Adv. Mater.*, 2017, **29**, 1602737.
72. W. Lewandowski, N. Vaupotič, D. Pociecha, E. Górecka and L. M. Liz-Marzán, *Adv. Mater.*, 2020, **32**, 1905591.
73. K. Ariga, T. Mori, T. Kitao and T. Uemura, *Adv. Mater.*, 2020, **32**, 1905657.
74. N. Sebastián, N. Gimeno, J. Vergara, D. O. López, J. L. Serrano, C. L. Folcia, M. R. de la Fuente and M. B. Ros, *J. Mater. Chem. C*, 2014, **2**, 4027-4036.
75. N. Gimeno, J. Vergara, M. Cano, J. Luis Serrano, M. Blanca Ros, J. Ortega, C. L. Folcia, S. Rodriguez-Conde, G. Sanz-Enguita and J. Etxebarria, *Chem. Mater.*, 2013, **25**, 286-296.
76. M. Castillo-Vallés, M. Cano, A. Bermejo-Sanz, N. Gimeno and M. B. Ros, *J. Mater. Chem. C*, 2020, **8**, 1998-2007.
77. C. Keith, R. A. Reddy, A. Hauser, U. Baumeister and C. Tschierske, *J. Am. Chem. Soc.*, 2006, **128**, 3051-3066.
78. W.-H. Chen, W.-T. Chuang, U. S. Jeng, H.-S. Sheu and H.-C. Lin, *J. Am. Chem. Soc.*, 2011, **133**, 15674-15685.
79. R. A. Reddy, C. Zhu, R. Shao, E. Korblova, T. Gong, Y. Shen, E. Garcia, M. A. Glaser, J. E. Maclennan, D. M. Walba and N. A. Clark, *Science*, 2011, **332**, 72-77.

80. E. Westphal, H. Gallardo, G. F. Caramori, N. Sebastián, M.-G. Tamba, A. Eremin, S. Kawauchi, M. Prehm and C. Tschierske, *Chem. Eur. J.*, 2016, **22**, 8181-8197.
81. E. Westphal, H. Gallardo, N. Sebastián, A. Eremin, M. Prehm, M. Alaasar and C. Tschierske, *J. Mater. Chem. C*, 2019, **7**, 3064-3081.
82. J. Vergara, J. Barberá, J. L. Serrano, M. B. Ros, N. Sebastián, R. de la Fuente, D. O. López, G. Fernández, L. Sánchez and N. Martín, *Angew. Chem. Int. Ed.*, 2011, **50**, 12523-12528.
83. M. Pfletscher, S. Hölscher, C. Wölper, M. Mezger and M. Giese, *Chem. Mater.*, 2017, **29**, 8462-8471.
84. M. Cano, A. Sánchez-Ferrer, J. L. Serrano, N. Gimeno and M. B. Ros, *Angew. Chem. Int. Ed.*, 2014, **53**, 13449-13453.
85. M. Castillo-Vallés, P. Romero, V. Sebastián and M. B. Ros, *Nanoscale Adv.*, 2021, **3**, 1682-1689.
86. D. Shen, A. Pegenau, S. Diele, I. Wirth and C. Tschierske, *J. Am. Chem. Soc.*, 2000, **122**, 1593-1601.
87. I. C. Pintre, N. Gimeno, J. L. Serrano, M. B. Ros, I. Alonso, C. L. Folcia, J. Ortega and J. Etxebarria, *J. Mater. Chem.*, 2007, **17**, 2219-2227.
88. The S0→S1 is hardly visible due to the low oscillator strength, f around 0.002, see R. S. Becker, I. S. Singh, E. A. Jackson, *J. Chem. Phys.* 1963, **38**, 2144-2171.
89. In deaerated solution, the quantum yields are around 30%; see W. R. Dawson, M. W. Windsor, *J. Phys. Chem.* 1968, *72*, 3251-3260..
90. Birks suggested to define an excimer as "a molecular dimer or stoichiometric complex which is associated in an excited electronic state and which is dissociative (i.e., dissociates in the absence of external restraints) in its electronic ground state"; see J. B. Birks, in The Exciplex (Eds: M. Gordon, W. R. Ware), Academic Press, New York 1975, p. 39.
91. S. K. Behera, S. Y. Park and J. Gierschner, *Angew. Chem. Int. Ed.*, 2021, **60**, 22624-22638.
92. S. Farid, P. A. Martic, R. C. Daly, D. R. Thompson, D. P. Specht, S. E. Hartman and J. L. R. Williams, *Pure Appl. Chem.* , 1979, **51**, 241.
93. A. Warshel and E. Huler, *Chem. Phys.*, 1974, **6**, 463-468.
94. F. Hirayama, *J. Chem. Phys.*, 1965, **42**, 3163-3171.
95. J. Gierschner, H.-G. Mack, D. Oelkrug, I. Waldner and H. Rau, *J. Phys. Chem. A*, 2004, **108**, 257-263.
96. S. Reiter, M. K. Roos and R. de Vivie-Riedle, *ChemPhotoChem*, 2019, **3**, 881-888.
97. For an ideal side-by-side arrangement of a dimer, the simple electronic exciton model predicts a zero oscillator strength *f*; static and dynamic symmetry breaking then gives rise to little, but non-zero *f*. The resulting *f* is directly proportional to k_F via the Strickler-Berg relation; see S. J. Strickler, R. A. Berg, *J. Chem. Phys.* 1962, **37**, 814-822.
98. J. Gierschner, J. Shi, B. Milián-Medina, D. Roca-Sanjuán, S. Varghese and S. Park, *Adv. Opt. Mater.*, 2021, **9**, 2002251.
99. R. Katoh, K. Suzuki, A. Furube, M. Kotani and K. Tokumaru, *J. Phys. Chem. C*, 2009, **113**, 2961-2965.
100. J. Shi, L. E. Aguilar Suarez, S.-J. Yoon, S. Varghese, C. Serpa, S. Y. Park, L. Lüer, D. Roca-Sanjuán, B. Milián-Medina and J. Gierschner, *J. Phys. Chem. C*, 2017, **121**, 23166-23183.
101. It is noted that also reabsorption contributes to non-exponential lifetimes in molecular solids; this was however largely avoided in the experiments by effectively reducing light penetration, see e.g. Ref. 97.
102. K. Lalitha and S. Nagarajan, *J. Mater. Chem. B*, 2015, **3**, 5690-5701.
103. D. Kraskouskaya, M. Bancerz, H. S. Soor, J. E. Gardiner and P. T. Gunning, *J. Am. Chem. Soc.*, 2014, **136**, 1234-1237.
104. N. Prigyai, S. Chanmungkalakul, S. Thanyalax, M. Sukwattanasinitt and V. Ervithayasuporn, *Materials Adv.*, 2020, **1**, 3358-3368.
105. S. Mondal, P. Bairi, S. Das and A. K. Nandi, *J. Mater. Chem. A*, 2019, **7**, 381-392.
106. D. Chen, C. Zhu, H. Wang, J. E. Maclennan, M. A. Glaser, E. Korblova, D. M. Walba, J. A. Rego, E. A. Soto-Bustamante and N. A. Clark, *Soft Matter*, 2013, **9**, 462-471.
107. A. Zep, M. Salamonczyk, N. Vaupotič, D. Pociecha and E. Gorecka, *Chem. Commun.*, 2013, **49**, 3119-3121.
108. T. G. Barclay, K. Constantopoulos and J. Matisons, *Chem. Rev.*, 2014, **114**, 10217-10291.
109. A. Nitti, A. Pacini and D. Pasini, *Nanomaterials*, 2017, **7**, 167.
110. V. Novotná, V. Hamplová, L. Lejček, D. Pociecha, M. Cigl, L. Fekete, M. Glogarová, L. Bednárová, P. W. Majewski and E. Gorecka, *Nanoscale Adv.*, 2019, **1**, 2835-2839.
111. T. Shimizu, W. Ding and N. Kameta, *Chem. Rev.*, 2020, **120**, 2347-2407.